JOURNAL OF AGRICULTURAL AND FOOD CHEMISTRY
ARTICLE

J. Agric. Food Chem. 2010, 58, 5561–5567 5561
DOI:10.1021/jf100412q

Impact of Carbon Chain Length on Binding of Perfluoroalkyl Acids to Bovine Serum Albumin Determined by Spectroscopic Methods

Pengfei Qin, Rutao Liu,* Xingren Pan, Xiaoyan Fang, and Yue Mou

School of Environmental Science and Engineering, Shandong University. China−America Cooperative Research Center for Environment and Health of Shandong Province, 27 Shanda South Road, Jinan 250100, People's Republic of China

Perfluoroalkyl acids (PFAAs), an emerging class of globally environmental contaminants, pose a great threat to humans with wide exposure from food and other potential sources. To evaluate the toxicity of PFAAs at the protein level, the effects of three PFAAs on bovine serum albumin (BSA) were characterized by fluorescence spectroscopy, synchronous fluorescence spectroscopy, and circular dichroism (CD). On the basis of the fluorescence spectra and CD data, we concluded that perfluoropentanoic acid (PFPA) had little effect on BSA. However, perfluorooctanoic acid (PFOA) and perfluorodecanoic acid (PFDA) exhibited remarkable fluorescence quenching, which was attributed to the formation of a moderately strong complex. The enthalpy change (ΔH) and entropy change (ΔS) indicated that van der Waals forces and hydrogen bonds were the dominant intermolecular forces in the binding of PFAAs to BSA. Furthermore, the BSA conformation was slightly altered in the presence of PFOA and PFDA, with a reduction of α helix. These results indicated that PFAAs indeed impact the conformation of BSA, and PFAAs with longer carbon chains were more toxic, especially at lower concentrations.

KEYWORDS: Perfluoroalkyl acids (PFAAs); bovine serum albumin (BSA); fluorescence; toxicological evaluation

INTRODUCTION

Perfluoroalkyl acids (PFAAs) are a family of synthetic perfluorinated chemicals that are composed of a carbon backbone typically 4−14 atoms in length and a charged functional group (primarily carboxylate, sulfonate, or phosphonate). The eight-carbon molecules known as perfluorooctanoic acid (PFOA) and perfluorooctane sulfonate (PFOS) are two of the most common representatives. The unique chemical properties of PFAAs (*1*) make them highly desirable in the manufacture of a variety of products, such as fabrics, floor waxes, polymeric products, food packaging, and industrial surfactants (*2*, *3*).

The carbon−fluorine bond is one of the strongest bonds in organic chemistry; thus, these fully fluorinated hydrocarbons are exceedingly stable and resistant to degradation by natural processes, such as metabolism, hydrolysis, photolysis, or biodegradation. PFAAs have been identified at low concentrations in environmental media samples, wildlife, and even humans (*4*−*7*). Because of their broad exposures in the environment, many studies have been performed to evaluate their potential human health effects (*8*−*10*). The treatment of rodents with PFOA and PFOS can cause reductions in body weight, peroxisomal β-oxidation in cultured hepatocytes, and decreases in serum cholesterol and triglycerides (*11*, *12*). In addition, PFAAs with various alkyl chain lengths show major differences in their toxic effects. The rate of elimination is enhanced for short carbon chain lengths, while PFAAs with longer chains are more bioaccumulative according to the biomonitoring data (*13*, *14*). However, their distributions are different from other persistent organic pollutants (POPs), which accumulate in human adipose tissue. Interestingly, PFAAs are accumulated mainly in plasma, liver, and kidney because of their hydrophilic nature (*15*). In recent years, considerable public attention has been paid more to the toxicities of PFOA and PFOS because of their wide distribution (*16*, *17*), yet the lack of toxicological data for other PFAAs still greatly limits risk assessment of the environmental pollution caused by PFAAs. Previous studies have shown that these perfluoroalkyl chemicals could interfere with the binding affinity of fatty acids with liver−fatty acid binding protein (*18*). Besides, they are suspected to be circulated throughout the body by noncovalent binding to plasma proteins primarily with serum albumins (*15*). However, there are few detailed studies on the protein binding properties and potential toxicological relationship of PFAAs in the same class, which are potentially important for understanding and predicting the toxicity of PFAAs in the human plasma.

Serum albumins are the major soluble proteins of the circulatory system and have many physiological functions. They serve as a depot protein and play important roles in the transportation

*To whom correspondence should be addressed: School of Environmental Science and Engineering, Shandong University, Jinan 250100, People's Republic of China. Telephone/Fax: 86-531-88364868. E-mail: rutaoliu@sdu.edu.cn.

Published on Web 04/19/2010

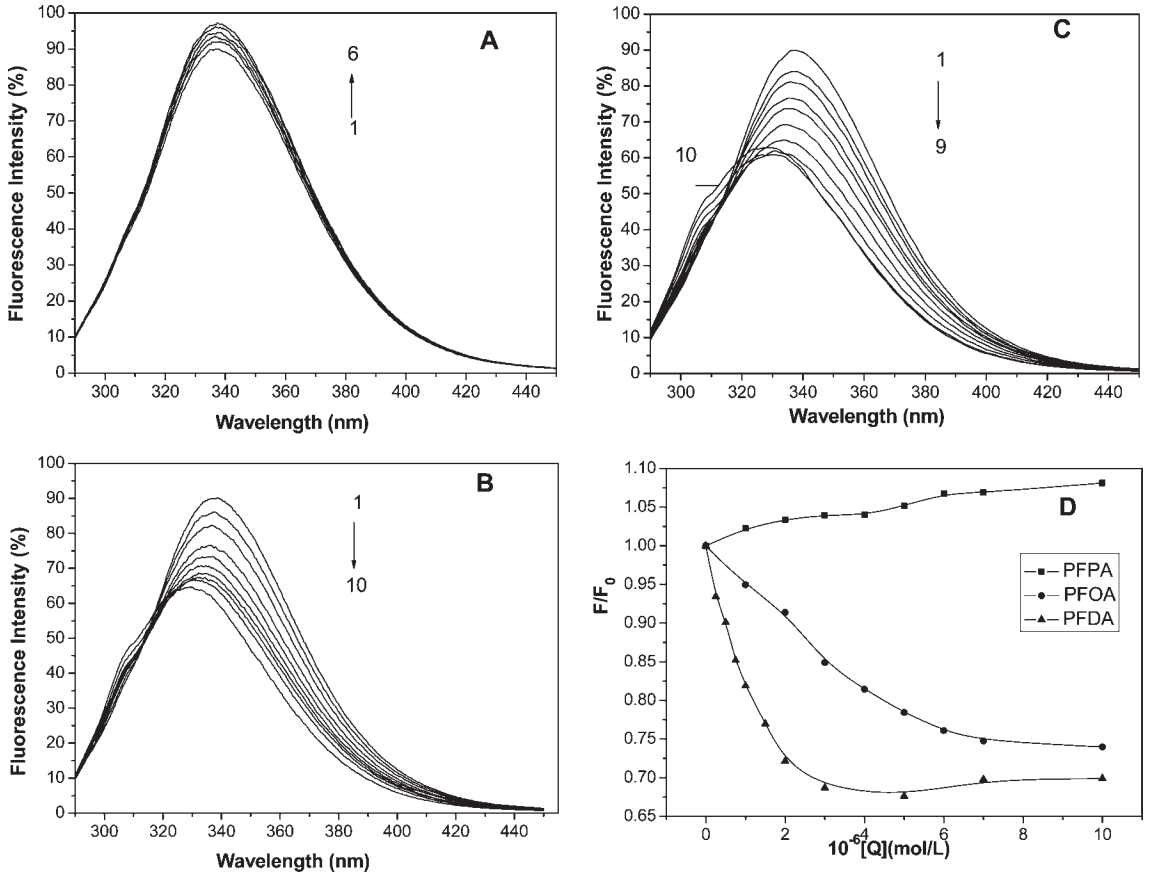

Figure 1. Effect of (A) PFPA, (B) PFOA, (C) PFDA on the fluorescence intensity of BSA; (D) Normalized fluorescence intensity of BSA with (■) PFPA, (●) PFOA and (▲) PFDA concentrations. PFPA ($\times 10^{-6}$ mol/L) 1−6: 0, 1, 3, 5, 7, and 10. PFOA ($\times 10^{-6}$ mol/L) 1−10: 0, 1, 2, 3, 4, 5, 6, 7, 10, and 20. PFDA ($\times 10^{-6}$ mol/L) 1−10: 0, 0.25, 0.5, 0.75, 1, 1.5, 2, 3, 5, and 7. The concentration of BSA: 1×10^{-6} mol/L; Buffer: NaH_2PO_4−Na_2HPO_4, pH = 7.40; T = 300 K.

of a variety of endogenous and exogenous compounds in blood (*19*). It has been proposed that the distribution and metabolism of many biologically active compounds, such as metabolites, drugs, and even some toxins, in the body are correlated with their affinities toward serum albumin (*20*, *21*). The binding of toxicants to serum albumin can impede the transport of endogenous substances and cause conformational changes of protein, which may affect its activity or even change its physiological function (*22*, *23*). Because of its structural homology with human serum albumin (HSA), bovine serum albumin (BSA) has been one of the most extensively studied members of this group of proteins (*24*).

Fluorescence has been proven as a sensible method to provide qualitative and quantitative information on the PFAA−albumin interactions, especially at low PFAA concentrations (*25*). Therefore, in this work, we use fluorescence spectroscopy, synchronous fluorescence, and circular dichroism (CD) techniques to explore the toxic effects of perfluoropentanoic acid (PFPA), PFOA, and perfluorodecanoic acid (PFDA) on BSA under simulative physiological conditions. The mechanisms of interaction of PFAAs with different carbon chain lengths to BSA, such as their binding constants and the impact on the conformational space, are discussed. This report provides a new approach to explore the biological toxicity of PFAAs at the functional macromolecular level. In addition, it will also complement studies on the environmental risk assessment of PFAA pollution.

MATERIALS AND METHODS

Reagents. BSA (electrophoretic grade reagent, 90% purity) purchased from Beijing Chemical Reagent Corporation was prepared at 1.0×10^{-5} mol/L in 0.02 mol/L NaH_2PO_4−Na_2HPO_4 (pH 7.40), then preserved at 0−4 °C, and diluted as required. PFPA (97% purity), PFOA (95% purity), and PFDA (97% purity) were all purchased from Alfa Aesar (Ward Hill, MA). Stock solutions of PFPA, PFOA, and PFDA were prepared at a concentration of 1.0×10^{-3}, 1.0×10^{-3}, and 1.0×10^{-4} mol/L in 0.02 mol/L NaH_2PO_4−Na_2HPO_4 (pH 7.40) buffer. All other chemicals were of analytical grade. Ultrapure water was used throughout the experiments.

Fluorescence Quenching Measurements. All fluorescence spectra were measured on a F-4600 fluorophotometer (Hitachi, Japan) equipped with a 10 mm quartz cell and a 150 W xenon lamp. A certain amount of PFAA and 1 mL of BSA stock solution were added in turn to a 10 mL colorimetric tube and made up to the mark with 0.02 mol/L NaH_2PO_4−Na_2HPO_4 (pH 7.40) buffer. After equilibration for 20 min, the fluorescence emission spectra were scanned in the range of 290−450 nm using an excitation wavelength of 278 nm at three temperatures. The excitation and emission slit widths were both set at 5 nm.

Principles of Fluorescence Quenching. Fluorescence quenching data are first analyzed with the Stern−Volmer equation(*26*)

$$F_0/F = 1 + K_{sv}[Q] = 1 + k_q\tau_0[Q] \quad (1)$$

where F_0 and F are the fluorescence intensities of protein in the absence and presence of the quencher, respectively, k_q is the quenching rate constant of the biomolecule, K_{sv} is the dynamic quenching constant, τ_0 is average lifetime of the molecule without the quencher and is generally taken as 10^{-8} s, and $[Q]$ is the concentration of the quencher.

Otherwise, the data should follow the modified Stern−Volmer equation (*26*) for static quenching

$$\frac{F_0}{\Delta F} = \frac{1}{f_a K_a}\frac{1}{[Q]} + \frac{1}{f_a} \quad (2)$$

where ΔF is the difference in fluorescence intensity with and without the quencher at concentration $[Q]$, K_a is the effective quenching constant for

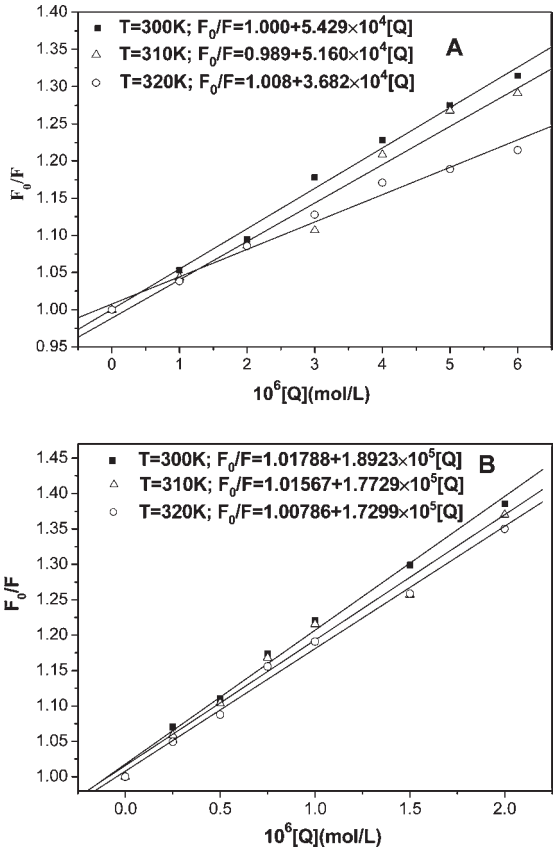

Figure 2. Stern−Volmer plots for (A) PFOA and (B) PFDA with BSA at (■) 300 K, (△) 310 K, and (○) 320 K. The concentration of BSA = 1 × 10^{-6} mol/L. Buffer = NaH_2PO_4−Na_2HPO_4 at pH 7.40.

Table 1. Stern−Volmer Quenching Constants of the PFOA−BSA and PFDA−BSA Systems at Different Temperatures

	T (K)	K_{sv} ($\times 10^4$ L mol^{-1})	k_q ($\times 10^{12}$ mol L^{-1} s^{-1})	R	SD
PFOA	300	5.43	5.43	0.99587	0.01171
	310	5.16	5.16	0.98562	0.02093
	320	3.68	3.68	0.99142	0.01149
PFDA	300	18.92	18.92	0.99599	0.01313
	310	17.73	17.73	0.9909	0.0186
	320	17.30	17.30	0.99646	0.01128

the accessible fluorophores, and f_a is the fraction of accessible fluorescence. The dependence of $F_0/\Delta F$ on the reciprocal value of the quencher concentration $[Q]^{-1}$ is linear, with a slope equal to the value of $(f_a K_a)^{-1}$.

As for the temperature-dependent thermodynamic parameters, they could be studied on the basis of the van't Hoff equation (*27*), if the enthalpy change (ΔH) does not vary significantly over a certain temperature range

$$\ln K = -\frac{\Delta H}{RT} + \frac{\Delta S}{R} \quad (3)$$

where K is analogous to the effective quenching constants K_a at the corresponding temperature and R is the gas constant. In addition, the free energy change (ΔG) can be estimated according to the following relationship:

$$\Delta G = \Delta H - T\Delta S = -RT \ln K \quad (4)$$

CD Studies. CD spectra of BSA in the absence and presence of PFAAs were taken over the range of 200−250 nm on a J-810 CD spectrometer (Jasco, Tokyo, Japan) using a quartz cell with a path length of 10 mm. The scanning speed was set at 200 nm/min. Each spectrum was the average of two successive scans.

The CD results were expressed in terms of mean residue ellipticity (MRE) in degree cm^2 dmol^{-1} according to the following equation (*28*):

$$\text{MRE} = \frac{\text{observed CD (medg)}}{C_p n l \times 10} \quad (5)$$

$$\alpha \text{ helix } (\%) = \frac{-\text{MRE}_{208} - 4000}{33000 - 4000} \times 100 \quad (6)$$

where C_p is the molar concentration of the protein, n is the number of amino acid residues, and l is the path length.

RESULTS AND DISCUSSION

Fluorescence Quenching Spectra of BSA. BSA is considered to possess intrinsic fluorescence originating from the Trp-134 and Trp-212 tryptophan residues. Trp-212 is situated within a hydrophobic binding pocket of the protein, which is in a well-characterized binding cavity for small charged aromatic molecules, while Trp-134 is thought to be located on the surface of the molecule (*19*). Consequently, fluorescence quenching can be regarded as a technique for the measurement of binding affinities.

The fluorescence spectra of BSA at a series of concentrations of PFPA, PFOA, and PFDA at 300 K are illustrated in **Figure 1**. As shown in **Figure 1A**, the fluorescence intensity is slightly enhanced by the addition of PFPA but there is no shift of the emission wavelength. In contrast, the spectra of the other two systems, PFOA−BSA and PFDA−BSA, manifest remarkable fluorescence quenching as the concentration increases (panels **B** and **C** of **Figure 1**). Concomitantly, their emission peak wavelengths significantly blue shift, which is attributed to the increased hydrophobicity around tryptophan residues. The drop of fluorescence can be rationalized by the conformational changes of BSA after the binding, which can lead to the gradual exposure of tryptophan residues to water. To make the trends more clear, the normalized fluorescence F/F_0 of the spectra is plotted in **Figure 1D** as a function of the PFAA concentration, where F_0 and F are the fluorescence intensities of BSA before and after the addition of PFAAs, respectively. When the general trends of the three curves in **Figure 1D** are compared, the slight rise of the PFPA curve indicates that PFPA has little effect on the fluorescence intensity of BSA. However, the other two compounds exhibit significant drops in a certain range and then become steady at higher concentrations. From the slopes of the PFOA and PFDA curves, it can be concluded that the binding of PFDA to BSA is much stronger than that of PFOA. In other words, PFDA could pose more of a health threat than PFOA at lower exposures. Our further research below into the mechanism of fluorescence quenching was limited to PFOA and PFDA.

Mechanisms of Fluorescence Quenching. Fluorescence quenching is the decrease of the quantum yield of fluorescence from a fluorophore induced by a variety of molecular interactions with quencher molecules. The different mechanisms of fluorescence quenching are usually classified as either dynamic quenching, resulting from collisional encounters, or static quenching, because of the formation of a ground-state complex between the fluorophore and quencher. In both cases, molecular contact is required between the fluorophore and the quencher for fluorescence quenching to occur (*26*). Yet the two forms of fluorescence quenching can be distinguished by their different dependence upon temperature and viscosity or preferably by lifetime measurements.

To further elucidate the quenching mechanism induced by PFAAs, the graphs plotted for F_0/F against $[Q]$ according to the Stern−Volmer equation are shown in **Figure 2**. The curves are

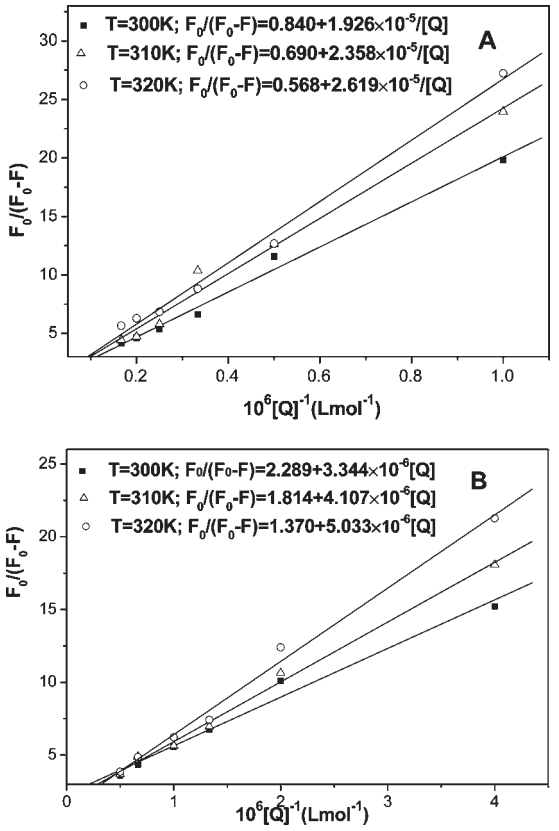

Figure 3. Modified Stern−Volmer plots for (A) PFOA and (B) PFDA with BSA at (■) 300 K, (△) 310 K, and (○) 320 K. The concentration of BSA = 1×10^{-6} mol/L. Buffer = NaH_2PO_4−Na_2HPO_4 at pH 7.40.

Table 2. Modified Stern−Volmer Association Constants K_a and Relative Thermodynamic Parameters of the PFOA−BSA and PFDA−BSA Systems

reagents	T (K)	K_a ($\times 10^4$ mol L^{-1})	R	ΔH (kJ mol^{-1})	ΔG (kJ mol^{-1})	ΔS (J (mol^{-1} K^{-1})
PFOA	300	4.36	0.99497	−27.61	−26.61	−3.32
	310	2.93	0.99181		−26.58	
	320	2.17	0.9967		−26.55	
PFDA	300	68.46	0.99155	−37.14	−33.55	−11.96
	310	44.17	0.99744		−33.43	
	320	27.22	0.99658		−33.31	

linear with high R values, and the calculated quenching constants at the corresponding temperatures are listed in **Table 1**.

Generally speaking, during the dynamic process, the quenching rate constants of the fluorescent complexes will increase with the temperature, because the higher temperatures will result in faster diffusion and, hence, lead to larger amounts of collision quenching. Moreover, the maximum dynamic quenching constant k_q of the various quenchers is 2.0×10^{10} L mol^{-1} s^{-1} under normal circumstances (*26*). However, the constant K_{sv} in **Table 1** is inversely correlated with the temperature, and k_q is much larger than 2.0×10^{10} L mol^{-1} s^{-1}. Therefore, we preliminarily conclude that the quenching mechanisms belong to static quenching.

The modified Stern−Volmer plots are displayed in **Figure 3**, and the corresponding values of K_a at three temperatures are presented in **Table 2**. The quenching constants are found to decrease as the temperature rises. Therefore, the data again confirm that the quenching process between BSA and PFAAs belongs to static quenching.

Thermodynamic Parameters and Binding Modes. There are four types of interactions between small molecule ligands and biological macromolecules: hydrophobic forces, hydrogen bonds,

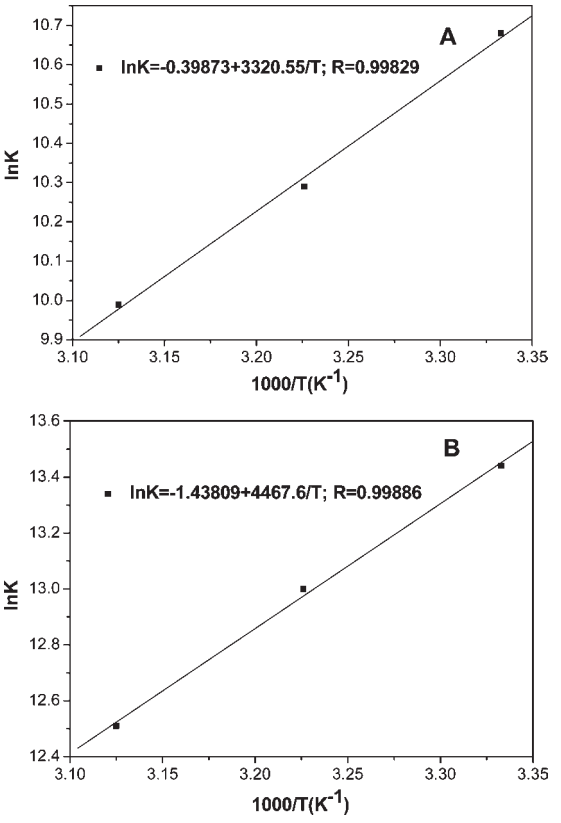

Figure 4. van't Hoff plot for the interaction of BSA with (A) PFOA and (B) PFDA in phosphate buffer.

van der Waals forces, and electrostatic interactions. The signs and magnitudes of the thermodynamic parameters (ΔH and ΔS) can account for the main forces involved in the binding reaction. If the temperature changes little, the reaction enthalpy change (ΔH) can be regarded as constant and can be calculated on the basis of the slope of a plot of ln K versus $1/T$ (**Figure 4**).

Ross and Subramanian (*27*) have summed up the thermodynamic laws to determine the types of binding associated with various interactions. That is, if $\Delta H < 0$ and $\Delta S < 0$, van der Waals interactions and hydrogen bonds play main roles in the binding reaction. If $\Delta H > 0$ and $\Delta S > 0$, hydrophobic interactions are dominant. Electrostatic forces are more important when $\Delta H < 0$ and $\Delta S > 0$. The thermodynamic parameters and K_a values of the PFOA−BSA and PFDA−BSA systems are listed in **Table 2**. The negative sign for free energy (ΔG) of the PFOA−BSA system (**Table 2**) indicates that the interaction process is spontaneous. In addition, the values of ΔH and ΔS for the binding reaction are −27.61 kJ mol^{-1} and −3.32 J mol^{-1} K^{-1}, respectively, which demonstrate that hydrogen bonds and van der Waals forces play major roles in the acting forces.

PFOA is known as a water and oil repellant (*1*, *2*). In aqueous solution, PFOA is lipophobic enough to insert into the hydrophobic cavity of BSA and the carboxylic acid can also form hydrogen bonds with the protein side chains. PFDA exhibits the same thermodynamic trends as PFOA, suggesting that hydrogen bonding and van der Waals forces are predominant in the binding of both molecules to BSA.

In addition, the K_a (**Table 2**) of PFDA−BSA is much greater than that of PFOA−BSA, revealing that PFDA, which has a longer carbon chain, has a higher affinity than PFOA, which is in accordance with the results in **Figure 1D**.

Conformational Changes Shown by Synchronous Fluorescence. Spectroscopy is considered to be an ideal tool to observe

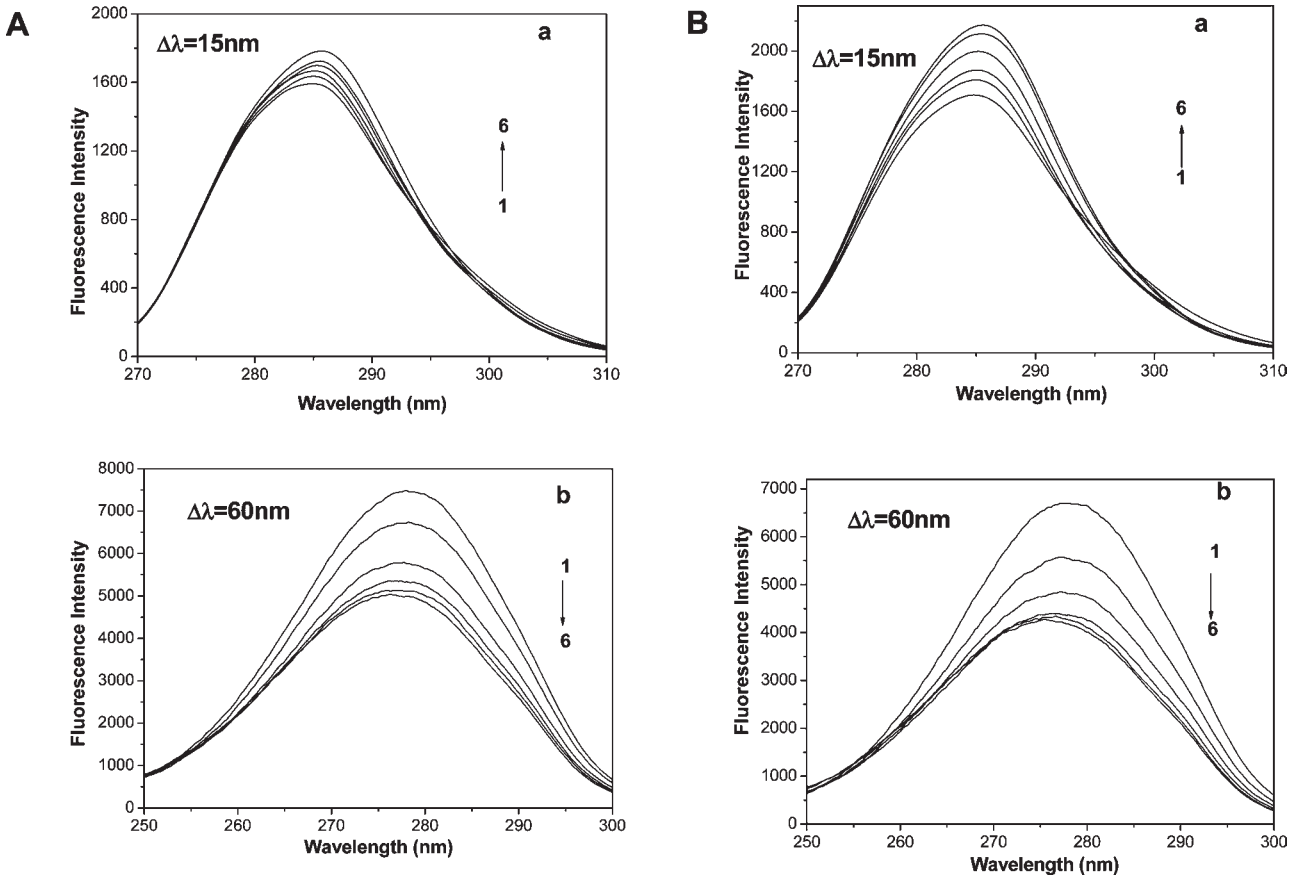

Figure 5. Synchronous fluorescence spectra of (A) PFOA and (B) PFDA with BSA: (a) observing tyrosine residues as $\Delta\lambda$ = 15 nm and (b) observing tryptophan residues at $\Delta\lambda$ = 60 nm. (A) PFOA ($\times 10^{-6}$ mol/L) 1−6: 0, 1, 3, 5, 7, and 10. (B) PFDA ($\times 10^{-6}$ mol/L) 1−6: 0, 1, 2, 3, 5, and 7. The concentration of BSA = 1 $\times$ 10^{-6} mol/L. Buffer = NaH_2PO_4−Na_2HPO_4 at pH 7.40. T = 300 K.

structural and conformational changes, because it allows non-intrusive measurements of substances in low concentration under physiological conditions. The intrinsic fluorophores in serum albumins show significant advantages, because tryptophan is highly sensitive to the local environment and also displays a substantial spectral shift. As a result, the position of the spectra maximum (λ_{max}) depends upon the properties of the environment of the tryptophanyl residues, and the fluorescence spectra depend upon the degree of exposure of the tryptophanyl side chain to the polar aqueous solvent and its proximity to specific quenching groups (*26*, *29*).

Synchronous fluorescence spectra can supply characteristic information about the molecular environment in the vicinity of chromosphere molecules, such as tyrosine or tryptophan residues, and have several advantages, such as spectral simplification, reduction of the spectral bandwidth, and avoidance of different perturbing effects (*29*). Besides, the synchronous spectra are obtained through the simultaneous scanning of the excitation and the fluorescence monochromators of a fluorimeter with a fixed wavelength difference ($\Delta\lambda$) between them. Therefore, synchronous fluorescence spectroscopy focusing on the tyrosine and tryptophan residues of BSA was adopted to explore the structural changes of BSA in the presence of various concentrations of PFOA and PFDA.

It is apparent from **Figure 5b** that the emission peaks of the tryptophan residues ($\Delta\lambda$ = 60 nm) show a slight blue shift upon the addition of PFOA and PFDA. This phenomenon expresses the conformational changes of the tryptophan residues, around which the polarity is decreased and the hydrophobicity is increased (*30*). Tyrosine ($\Delta\lambda$ = 15 nm) reveals the opposite intensity trend from tryptophan ($\Delta\lambda$ = 60 nm), showing a rise in intensity but no shift with the addition of PFAAs. These results further confirm that conformational and micro-environmental changes occur in BSA in the presence of PFAAs.

Secondary Structural Changes of BSA Shown by CD. CD is a powerful technique to investigate the secondary structural changes of proteins, because in the far-ultraviolet region, they are related to the polypeptide backbone structure (*31*). There are two negative peaks in the UV region at 208 and 222 nm, which are characteristic of the α-helical structure of a protein.

CD experiments at various concentrations of PFOA (**Figure 6A**) and other ones on all three PFAAs at the same concentration (**Figure 6B**) show the possible impact of PFAAs on the secondary structure of BSA. In **Figure 6A**, the proportion of α helix decreases gradually with the concentration of PFOA. In **Figure 6B**, the amount of α helix drops somewhat with the increase of the carbon chain lengths. From the curves in **Figure 6B**, there is little α-helix change in the PFPA−BSA system, indicating that PFPA has little effect on the conformation of BSA, consistent with the conclusion drawn from the fluorescence spectra. The other two PFAAs cause a decrease in α-helix content, and PFDA leads to a greater change than PFOA. All of these data confirm that the binding of PFAAs to BSA results in a change of the secondary structure of the protein.

In conclusion, serum albumin is known as a multifunctional plasma carrier protein for its ability to bind a wide variety of ligands (*24*). Tests of the potential damage of PFAAs with different carbon lengths to BSA were conducted at the molecular level by spectroscopic methods. PFAAs with a greater number of carbon atoms cause a stronger fluorescence quenching. PFPA was found to have little effect on BSA based on both the

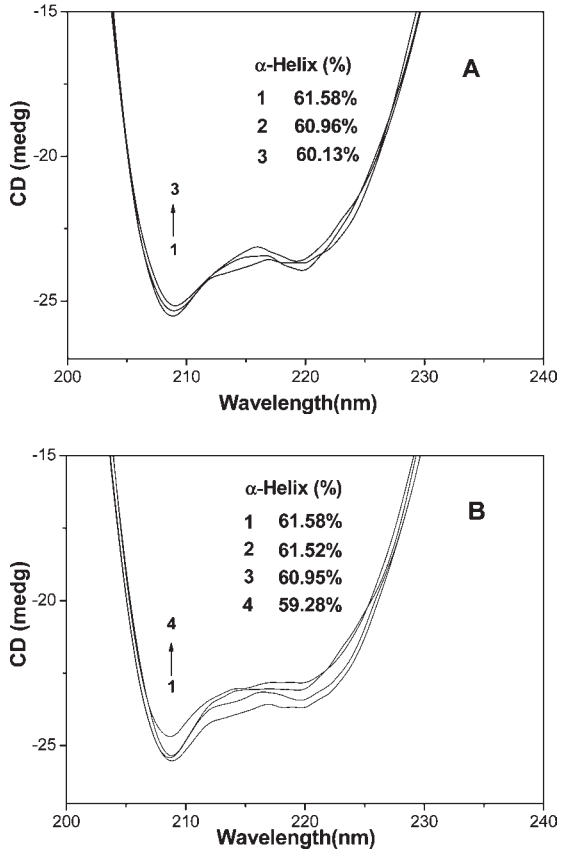

Figure 6. (A) CD spectra of (1) free BSA, (2) PFOA (2×10^{-6} mol/L) + BSA, and (3) PFOA (4×10^{-6} mol/L) + BSA. (B) CD spectra of (1) free BSA, (2) PFPA (1×10^{-6} mol/L) + BSA, (3) PFOA (1×10^{-6} mol/L) + BSA, and (4) PFDA (1×10^{-6} mol/L) + BSA. The concentration of BSA = 2×10^{-7} mol/L. Buffer = NaH_2PO_4−Na_2HPO_4 at pH 7.40. T = 300 K.

fluorescence spectra and CD data. PFOA and PFDA displayed static quenching on the fluorescence of BSA, which was produced by the spontaneous formation of a moderately strong complex with BSA. On the basis of the thermodynamic parameters, hydrogen bonding and van der Waals interactions played major roles in the binding of PFAAs to BSA. In addition, PFDA was found to bind more strongly than PFOA. Furthermore, the CD spectra confirmed that their binding could induce conformational changes to BSA. These results demonstrate that the chain length of PFAA has a profound impact on its binding affinity with BSA. The data can supply some quantitative information for studies on the molecular toxicology of the chain length and functional group of this class of compounds. Further studies are needed to provide a sound basis for health risk assessment of these chemicals.

ABBREVIATIONS USED

PFAA, perfluoroalkyl acid; PFPA, perfluoropentanoic acid; PFOA, perfluorooctanoic acid; PFDA, perfluorodecanoic acid; BSA, bovine serum albumin; CD, circular dichroism.

ACKNOWLEDGMENT

The authors thank Dr. Pamela Holt for editing the manuscript.

LITERATURE CITED

(1) Lemal, D. M. Perspective on fluorocarbon chemistry. *J. Org. Chem.* **2004**, *69* (1), 1–11.

(2) Lehmler, H. J. Synthesis of environmentally relevant fluorinated surfactants—A review. *Chemosphere* **2005**, *58* (11), 1471–1496.

(3) Renner, R. Perfluorinated sources outside and inside. *Environ. Sci. Technol.* **2004**, *38* (5), 80A.

(4) Houde, M.; Martin, J. W.; Letcher, R. J.; Solomon, K. R.; Muir, D. C. Biological monitoring of polyfluoroalkyl substances: A review. *Environ. Sci. Technol.* **2006**, *40* (11), 3463–3473.

(5) Kim, S. K.; Kannan, K. Perfluorinated acids in air, rain, snow, surface runoff, and lakes: Relative importance of pathways to contamination of urban lakes. *Environ. Sci. Technol.* **2007**, *41* (24), 8328–8334.

(6) Kannan, K.; Corsolini, S.; Falandysz, J.; Fillmann, G.; Kumar, K. S.; Loganathan, B. G.; Mohd, M. A.; Olivero, J.; Van Wouwe, N.; Yang, J. H.; Aldoust, K. M. Perfluorooctanesulfonate and related fluorochemicals in human blood from several countries. *Environ. Sci. Technol.* **2004**, *38* (17), 4489–4495.

(7) Ericson, I.; Marti-Cid, R.; Nadal, M.; Van Bavel, B.; Lindstrom, G.; Domingo, J. L. Human exposure to perfluorinated chemicals through the diet: intake of perfluorinated compounds in foods from the Catalan (Spain) market. *J. Agric. Food Chem.* **2008**, *56* (5), 1787–1794.

(8) Olsen, G. W.; Butenhoff, J. L.; Zobel, L. R. Perfluoroalkyl chemicals and human fetal development: An epidemiologic review with clinical and toxicological perspectives. *Reprod. Toxicol.* **2009**, *27* (3−4), 212–230.

(9) Lau, C. Perfluoroalkyl acids: Recent activities and research progress. *Reprod. Toxicol.* **2009**, *27* (3−4), 209–211.

(10) Tittlemier, S. A.; Pepper, K.; Seymour, C.; Moisey, J.; Bronson, R.; Cao, X. L.; Dabeka, R. W. Dietary exposure of Canadians to perfluorinated carboxylates and perfluorooctane sulfonate via consumption of meat, fish, fast foods, and food items prepared in their packaging. *J. Agric. Food Chem.* **2007**, *55* (8), 3203–3210.

(11) Wolf, D. C.; Moore, T.; Abbott, B. D.; Rosen, M. B.; Das, K. P.; Zehr, R. D.; Lindstrom, A. B.; Strynar, M. J.; Lau, C. Comparative hepatic effects of perfluorooctanoic acid and WY 14,643 in PPAR-α knockout and wild-type mice. *Toxicol. Pathol.* **2008**, *36* (4), 632–639.

(12) Berthiaume, J.; Wallace, K. B. Perfluorooctanoate, perflouroctanesulfonate, and *N*-ethyl perfluorooctanesulfonamido ethanol; peroxisome proliferation and mitochondrial biogenesis. *Toxicol. Lett.* **2002**, *129* (1−2), 23–32.

(13) Kudo, N.; Suzuki-Nakajima, E.; Mitsumoto, A.; Kawashima, Y. Responses of the liver to perfluorinated fatty acids with different carbon chain length in male and female mice: In relation to induction of hepatomegaly, peroxisomal β-oxidation and microsomal 1-acylglycerophosphocholine acyltransferase. *Biol. Pharm. Bull.* **2006**, *29* (9), 1952–1957.

(14) Yeung, L. W.; Loi, E. I.; Wong, V. Y.; Guruge, K. S.; Yamanaka, N.; Tanimura, N.; Hasegawa, J.; Yamashita, N.; Miyazaki, S.; Lam, P. K. Biochemical responses and accumulation properties of long-chain perfluorinated compounds (PFOS/PFDA/PFOA) in juvenile chickens (*Gallus gallus*). *Arch. Environ. Contam. Toxicol.* **2009**, *57* (2), 377–386.

(15) Han, X.; Snow, T. A.; Kemper, R. A.; Jepson, G. W. Binding of perfluorooctanoic acid to rat and human plasma proteins. *Chem. Res. Toxicol.* **2003**, *16* (6), 775–781.

(16) Wu, L. L.; Gao, H. W.; Gao, N. Y.; Chen, F. F.; Chen, L. Interaction of perfluorooctanoic acid with human serum albumin. *BMC Struct. Biol.* **2009**, *9*, 31.

(17) Zhang, X.; Chen, L.; Fei, X. C.; Ma, Y. S.; Gao, H. W. Binding of PFOS to serum albumin and DNA: Insight into the molecular toxicity of perfluorochemicals. *BMC Mol. Biol.* **2009**, *10*, 16.

(18) Luebker, D. J.; Hansen, K. J.; Bass, N. M.; Butenhoff, J. L.; Seacat, A. M. Interactions of fluorochemicals with rat liver fatty acid-binding protein. *Toxicology* **2002**, *176* (3), 175–185.

(19) Papadopoulou, A.; Green, R. J.; Frazier, R. A. Interaction of flavonoids with bovine serum albumin: A fluorescence quenching study. *J. Agric. Food Chem.* **2005**, *53* (1), 158–163.

(20) Zhao, L.; Liu, R.; Zhao, X.; Yang, B.; Gao, C.; Hao, X.; Wu, Y. New strategy for the evaluation of CdTe quantum dot toxicity targeted to bovine serum albumin. *Sci. Total Environ.* **2009**, *407* (18), 5019–5023.

(21) Liu, R.; Sun, F.; Zhang, L.; Zong, W.; Zhao, X.; Wang, L.; Wu, R.; Hao, X. Evaluation on the toxicity of nanoAg to bovine serum albumin. *Sci. Total Environ.* **2009**, *407* (13), 4184–4188.

(22) Gulden, M.; Morchel, S.; Tahan, S.; Seibert, H. Impact of protein binding on the availability and cytotoxic potency of organochlorine pesticides and chlorophenols in vitro. *Toxicology* **2002**, *175* (1−3), 201–213.
(23) Soares, S.; Mateus, N.; Freitas, V. Interaction of different polyphenols with bovine serum albumin (BSA) and human salivary α-amylase (HSA) by fluorescence quenching. *J. Agric. Food Chem.* **2007**, *55* (16), 6726–6735.
(24) Ghosh, K. S.; Sen, S.; Sahoo, B. K.; Dasgupta, S. A spectroscopic investigation into the interactions of 3′-*O*-carboxy esters of thymidine with bovine serum albumin. *Biopolymers* **2009**, *91* (9), 737–744.
(25) MacManus-Spencer, L. A.; Tse, M. L.; Hebert, P. C.; Bischel, H. N.; Luthy, R. G. Binding of perfluorocarboxylates to serum albumin: A comparison of analytical methods. *Anal. Chem.* **2010**, *82* (3), 974–981.
(26) Zhang, Y. Z.; Zhou, B.; Zhang, X. P.; Huang, P.; Li, C. H.; Liu, Y. Interaction of malachite green with bovine serum albumin: Determination of the binding mechanism and binding site by spectroscopic methods. *J. Hazard. Mater.* **2009**, *163* (2−3), 1345–1352.
(27) Ross, P. D.; Subramanian, S. Thermodynamics of protein association reactions: Forces contributing to stability. *Biochemistry* **1981**, *20* (11), 3096–3102.
(28) Li, Y.; He, W.; Liu, J.; Sheng, F.; Hu, Z.; Chen, X. Binding of the bioactive component jatrorrhizine to human serum albumin. *Biochim. Biophys. Acta* **2005**, *1722* (1), 15–21.
(29) Lin, H.; Lan, J.; Guan, M.; Sheng, F.; Zhang, H. Spectroscopic investigation of interaction between mangiferin and bovine serum albumin. *Spectrochim. Acta, Part A* **2009**, *73* (5), 936–941.
(30) Guo, M.; Lu, W. J.; Li, M. H.; Wang, W. Study on the binding interaction between carnitine optical isomer and bovine serum albumin. *Eur. J. Med. Chem.* **2008**, *43* (10), 2140–2148.
(31) Zhang, H. X.; Gao, S.; Xiong, Z. Y.; Liu, S. P. Fluorometric probing on the binding of hematoxylin to serum albumin. *Mol. Biol. Rep.* **2009**, *36* (8), 2299–2306.

Received for review February 1, 2010. Revised manuscript received April 1, 2010. Accepted April 5, 2010. This work is supported by the National Natural Science Foundation of China (NSFC) (20875055), the Cultivation Fund of the Key Scientific and Technical Innovation Project, Ministry of Education of China (708058), NCET-06-0582, and the Foundation for Middle Young Scientists and Key Science and Technology Project in Shandong Province (2007BS08005 and 2008GG10006012).